Title:

Influence of process operating conditions on solvent thermal and oxidative degradation in post-combustion CO_2 capture

Correspondence author:

Grégoire Léonard

Address: Department of Applied Chemistry, University of Liège, Allée de la Chimie B6A, Liège, 4000, Belgium.

Tel.: 0032/4366 9592

Fax: 0032/4366 3525

E-Mail: g.leonard@ulg.ac.be

Influence of process operating conditions on solvent thermal and oxidative degradation in post-combustion CO₂ capture

Grégoire Léonard*, **Cyril Crosset, Dominique Toye, Georges Heyen**

[a]Department of Applied Chemistry, University of Liège, Allée de la chimie B6a, Liège Sart Tilman, 4000, Belgium.

* Corresponding author: Grégoire LEONARD, Department of Applied Chemistry, University of Liège, Allée de la Chimie B6a, Liège Sart Tilman, 4000, Belgium.
Phone: 0032 4366 9592
E-mail: g.leonard@ulg.ac.be

Abstract

The CO₂ post-combustion capture with amine solvents is modeled as a complex system interconnecting process energy consumption and solvent degradation and emission. Based on own experimental data, monoethanolamine degradation is included into a CO₂ capture process model. The influence of operating conditions on solvent loss is validated with pilot plant data from literature. Predicted solvent consumption rates are in better agreement with plant data than any previous work, and pathways are discussed to further refine the model. Oxidative degradation in the absorber is the largest cause of solvent loss while thermal degradation does not appear as a major concern. Using a single model, the process exergy requirement decreases by 10.8% and the solvent loss by 11.1% compared to our base case. As a result, this model provides a practical tool to simultaneously minimize the process energy requirement and the solvent consumption in post-combustion CO₂ capture plants with amine solvents.

Highlights:
1. Solvent degradation reactions are included into a global model of CO₂ capture
2. The model predicts same order of magnitude solvent loss compared to pilot plants
3. The influence of process operating parameters on degradation is quantified
4. Both energy requirement and solvent degradation are assessed using a single tool
5. Optimal operating conditions including flowsheet improvements are proposed

Keywords: Post-combustion CO₂ capture; monoethanolamine thermal and oxidative degradation; process modeling; plant design; integrated experimental and modeling study.

1.   Introduction

CO₂ capture and storage technologies represent one of the main technologies to rapidly reduce the anthropogenic emissions of carbon dioxide in response to the increasing environmental concerns and to the growing world energy demand. In 2011, 82% of the world energy demand was still generated from fossil fuels (IEA, 2013). Although this share is planned to decrease to 76% by 2035, fossil fuels are still the main source for energy in our society. Moreover, developing countries are pushing the demand for fossil fuels up. According to Bloomberg (2013), China will start operating one new 500 MW$_e$ coal power plant per week for the next 15 years! In this context, CO₂ capture, re-use and storage technologies (CCUS) are one of the most promising ways to significantly and rapidly reduce the emissions of anthropogenic greenhouse gases while addressing the increasing energy demand. Among existing CO₂ capture methods, the CO₂ post-combustion capture with amine solvents is the most mature for a large-scale deployment. It is based on an absorption – regeneration loop in which CO₂ from

the flue gas is absorbed into an amine solvent at temperatures varying between 40 and 60 °C. The process is usually designed so that the flue gas vented to the atmosphere after absorption contains 90 % less CO_2. The CO_2-loaded solvent is regenerated in a stripper at a higher temperature (between 100 and 140 °C, depending on the solvent). The produced CO_2 stream is almost pure and may be valorized (applications in food industry, enhanced oil recovery…) or stored underground. The present work studies the CO_2 capture in coal-fired power plants although it may be easily transposed to other applications.

In the last 15 years, many studies addressed the high energy requirement of the process which decreases the plant efficiency by about 30%. In particular, the influence of process operating conditions like the solvent flow rate and concentration, the stripper pressure and the column packing heights was studied by Freguia and Rochelle (2003). The influence of these parameters (at the exception of the packing heights) has also been studied by Abu Zahra et al. (2007a) with similar results. Alternative flowsheet configurations have also been intensely studied in order to reduce the process energy penalty. Among others, the absorber intercooling, the lean vapor compression, the split-flow configuration and the multi-pressure stripper have been modeled by Freguia and Rochelle (2003), Karimi et al. (2011a and 2011b) and Plaza et al. (2010). A detailed literature review of previous modeling studies with MEA and achieved results is available in Léonard (2013).

Besides the energy penalty of the process, the degradation of the amine solvent and its consequences represent the second main operational drawback of amine-based post-combustion CO_2 capture. First, the cost of the solvent make-up which is necessary to compensate for solvent losses may represent up to 22% of the process operational expenses according to Abu Zahra et al. (2007b). Then, the degradation of amine solvents leads to the formation of a large range of products that may modify the solvent properties and decrease the process efficiency, implying additional costs. Finally, the emission of amine solvents and volatile degradation products like ammonia or nitrosamines is a critical issue in CO_2 capture plants. Although emission reduction technologies exist (among others the (acid) water washing of the flue gas at the column outlet), the problem of volatile products emissions may still be significant in large-scale operating plants (Mertens et al., 2013).

So far, the process energy penalty and the degradation of amine solvents have been studied separately and published models of the CO_2 capture process did not consider solvent degradation at all. Only one significant model of the process taking solvent degradation into account has been proposed by Thong et al. (2012). This model is based on literature data for the degradation of 30 wt% monoethanolamine (MEA, the benchmark solvent for post-combustion CO_2 capture). However, this study relies on questionable assumptions regarding both experimental data and modeling assumptions, so this model did not lead to relevant results and it could not be validated to predict industrial scale degradation. Such a model is however essential for a proper process evaluation and design. Thus, the objective of the present work is to use an in-house model developed in Aspen Plus to assess the influence of process operating conditions on solvent degradation. In order to build this model, experimental data were collected using appropriate equipment and procedures developed at the University of Liège to accelerate solvent degradation (Léonard et al., 2014a) and the results of this experimental study are shortly recalled in Section 2. First, the relevance of accelerated conditions could be evidenced by reproducing in one-week lab experiments similar degradation pathways as observed in industrial CO_2 capture pilot plants over several months. Then, based on such accelerated conditions, the influence of the process operating parameters was experimentally studied, leading to a kinetic model for MEA oxidative and

thermal degradation (Léonard et al., 2014b) that was improved in (Léonard et al., 2014c) to take into account new experiments of MEA oxidative degradation in the absence of CO_2. Based on these results, an Aspen Plus model of the CO_2 post-combustion capture process that assesses solvent degradation is proposed and its main assumptions are discussed in Section 3. Finally, Section 4 presents the results of a simulation study using this model. The influences of key process operating parameters both on the energy requirement of the process and on its solvent consumption are quantified. The impact of flowsheet improvements is also studied and optimal conditions are proposed for the CO_2 capture process.

2.   Experimental study of solvent degradation

Solvent degradation is a slow phenomenon taking place over months in industrial capture plants. Thus, it was necessary to develop appropriate experimental equipment and procedures to accelerate solvent degradation within a reasonable timeframe at the lab scale. In the present study, the two main degradation pathways of MEA (oxidative degradation and thermal degradation of MEA with CO_2) are considered, while the MEA thermal decomposition and the reactions with flue gas contaminants like SO_x or NO_x have been neglected in a first approach. Indeed, thermal decomposition does not take place at the temperatures observed in CO_2 capture conditions and the presence of SO_x and NO_x may be considerably reduced, assuming a high efficiency of the flue gas cleaning steps occurring before the CO_2 capture.

Because it does not require the presence of a gas phase, thermal degradation with CO_2 was studied under batch conditions. On the contrary, oxidative degradation requires a continuous gas feed since it is limited by the rate of gas-liquid transfer (Goff, 2005). Thus, oxidative degradation experiments were conducted in an experimental Degradation Test Rig with continuous gas flow while the thermal degradation experiments with CO_2 were performed in batch cylinders. On the first side, the Degradation Test Rig for MEA oxidative degradation allows temperatures up to 140 °C and pressures up to 2 MPa, with flexible gas composition and variable agitation rate. Typically, 300 g of 30 wt% MEA (1.47 mol MEA and 11.67 mol H_2O) are weighted into the reaction vessel. The degradation experiment runs for one week at 120°C, 0.4 MPa (gauge) and 600 rpm with a continuous gas flow rate (160 NmL/min) composed of 5% O_2 and 95% N_2. After one week, the experiment is completed and a sample is taken for liquid analysis. On the other side, MEA thermal degradation was studied in batch reactors consisting of 150 ml-cylinders made of stainless steel 316L that were set into a laboratory oven. In a typical experimental run, the cylinders are filled with 100 g of the solvent to be tested, usually MEA 30 wt% that has been loaded with CO_2 to reach a loading of about 0.40 mol CO_2/mol MEA. Typical experiments run for 3 weeks at 140°C and a sample is taken every week for analysis. In order to characterize the degraded solvent samples, different analytical methods have been developed. The MEA content is determined by high performance liquid chromatography (HPLC) while liquid degradation products are quantified using gas chromatography (GC). Gaseous degradation products in the gas exhaust of the Degradation Test Rig are quantified on-line by Fourier transformed infra-red spectroscopy (FTIR). The nitrogen mass balance of degradation experiments could be closed within 10 % and repeatability was demonstrated with a deviation lower than 5 %. A detailed description of the equipment and procedures was published in a previous work (Léonard et al., 2014a).

Various degradation experiments were performed to study the influence of process operating variables on the degradation of 30 wt% MEA in water (benchmark solvent for CO_2 capture). Among other, the influence of the agitation rate, the temperature and the composition of the flue gas feed (varying concentrations in N_2, O_2 and CO_2) were tested. Identified degradation

pathways at lab-scale are observed to be similar to pathways observed in CO_2 capture pilot plants as evidenced in Figure 1 by the comparison of lab and industrial degraded solvent samples. The main products identified in Figure 1 are listed in the Appendix. Moreover, ammonia is the main degradation product identified in the gas phase. This study evidenced that oxidative degradation in the Degradation Test Rig is more representative of industrial degradation than thermal degradation in batch cylinders.
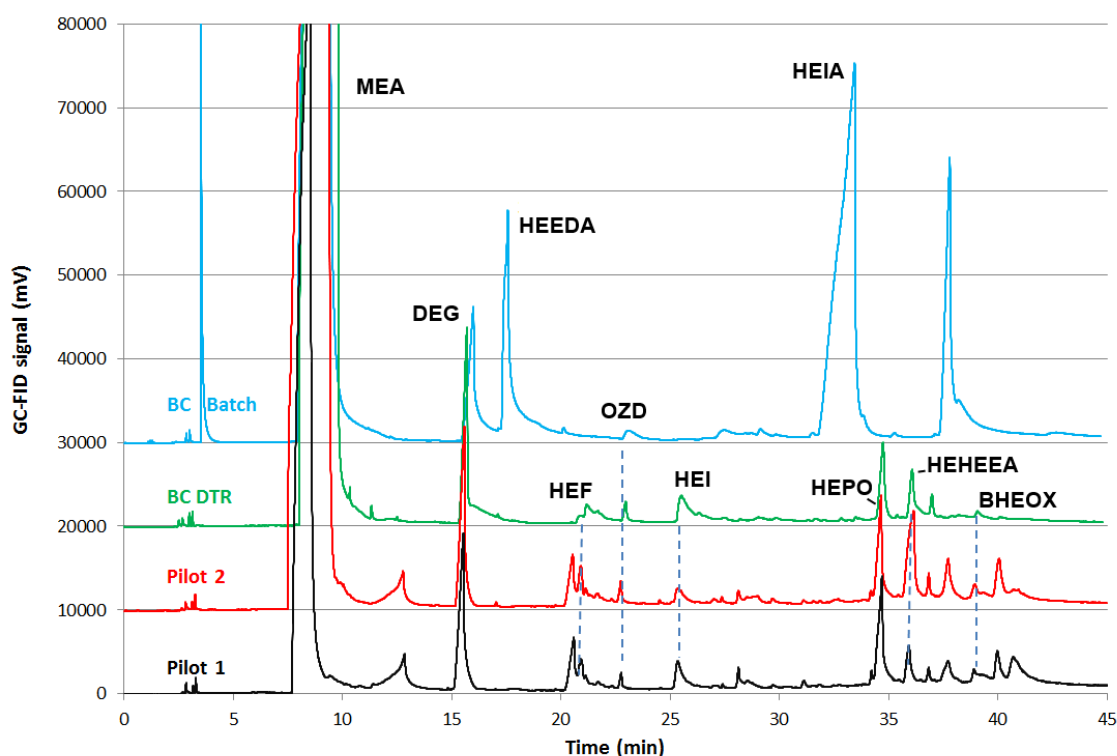

Figure1. Comparison of the gas chromatography spectra between lab experiments (base case) and degraded MEA samples from industrial pilot plants (Léonard et al., 2014a).

Based on the results of the degradation study, a kinetic model of MEA thermal and oxidative degradation was proposed, assuming one empirical degradation reaction for each studied degradation pathway. Since the exact reaction mechanisms of MEA oxidative degradation are still unknown, the stoichiometric coefficients of degradation products were determined from the product distribution observed in the experimental study and normalized to the degradation of one mol MEA. Although not measured in the present work, formic acid was included to take the formation of heat stable salts into account since they were identified in previous experimental studies (Sexton and Rochelle, 2009). The resulting apparent reaction of MEA with oxygen is given in Equation (1) while its kinetics is given in Equation (2) according to Arrhenius' equation. Regarding the thermal degradation of MEA with CO_2, degradation mechanisms are known and lead to Equation (3) with the associated kinetics from Equation (4). The reaction rates r are given in mol/(L.s). R is the universal gas constant (8.314 J/mol.K), T the temperature (K), and the MEA, O_2 and CO_2 concentrations are in mol/L. The values for the activation energies are given in J/mol. More details and results of the experimental degradation study are given in Léonard et al. (2014b) and Léonard et al. (2014c).

$$MEA + 1.3\ O_2 => 0.6\ NH_3 + 0.1\ HEI + 0.1\ HEPO + 0.1\ HCOOH + 0.8\ CO_2 + 1.5\ H_2O \qquad (1)$$

$$-r_{MEA, Oxidative} = 1.36 \ 10^6 . exp(-55 \ 111/RT) . [O_2]^{1.03} \tag{2}$$

$$MEA + 0.5 \ CO_2 => 0.5 \ HEIA + H_2O \tag{3}$$

$$-r_{MEA, Thermal} = 8.00 \ 10^{11} . exp(-144 \ 210/RT) . [CO_2] \tag{4}$$

3. Model description

This kinetic model for MEA oxidative and thermal degradation with CO_2 has been included into a global rate-based process model developed in Aspen Plus v8.6. Several steps were necessary to achieve the final flowsheet represented in Figure 2, some of them being described in Léonard and Heyen (2011) and in Léonard et al. (2013, 2014d). This model represents the pilot plant described by Knudsen et al. (2011), treating a flue gas flow rate of 5000 Nm³/h. The flue gas composition has been assumed to be that of a typical coal-fired power plant, i.e. 14% CO_2, 12% H_2O, 6% O_2, 68% N_2 (volume percentages). The flowsheet is represented in Figure 2. The lower part of the figure describes the absorption-regeneration loop of the CO_2 capture, while the upper part represents the CO_2 compression chain. Two virtual mixer blocs are added to sum up the cooling duty flows as well as the work flows.

The electrolyte non-random two-liquid (eNRTL) model is used for describing the liquid phase due to the presence of electrostatic interactions in the strongly non-ideal MEA-CO_2-Water system. The Redlich-Kwong (RK) equation of state is used for the vapor phase. However, the fluid exiting the CO2-COM3 compressor in the CO_2 compression chain is at a supercritical state and is cooled down by the CO2-HX3 heat exchanger to the liquid phase. As a consequence, a more adapted thermodynamic method has to be selected since the Redlich-Kwong equation of state is not appropriated for the determination of saturation pressures (vapor-liquid equilibria) at high pressures. Thus, the last three blocks of the CO_2 compression unit use the Peng-Robinson equation of state instead of the eNRTL-RK method.

The flue gas entering the process is first pre-cooled to 40°C in the PRECOOLE flash at atmospheric pressure. This precooling has two main purposes: it favors the exothermic CO_2 absorption and it helps regulating the process water balance. Then, the gas pressure is slightly increased by a blower before entering the 20-stage absorber. There, the gas is mixed with a 30 wt% MEA solution (flowing downwards from the column top) that absorbs the incoming CO_2. The CO_2 capture rate is adjusted by a design specification that varies the reboiler heat duty at the stripper (and thus the solvent lean loading) in order to reach 90% capture rate. The cleaned flue gas exiting the absorber is washed with water before being released to the atmosphere. The washing section of the absorber is modeled by an external 2-stage washing column. Most of the washing water is recycled to the top of the washer after cooling in the HX-WAS heat exchanger. The cooling temperature is set by a design specification in order to regulate and maintain the water balance of the CO_2 capture unit. A part of the excess water is recycled from the washing loop into the solvent loop.
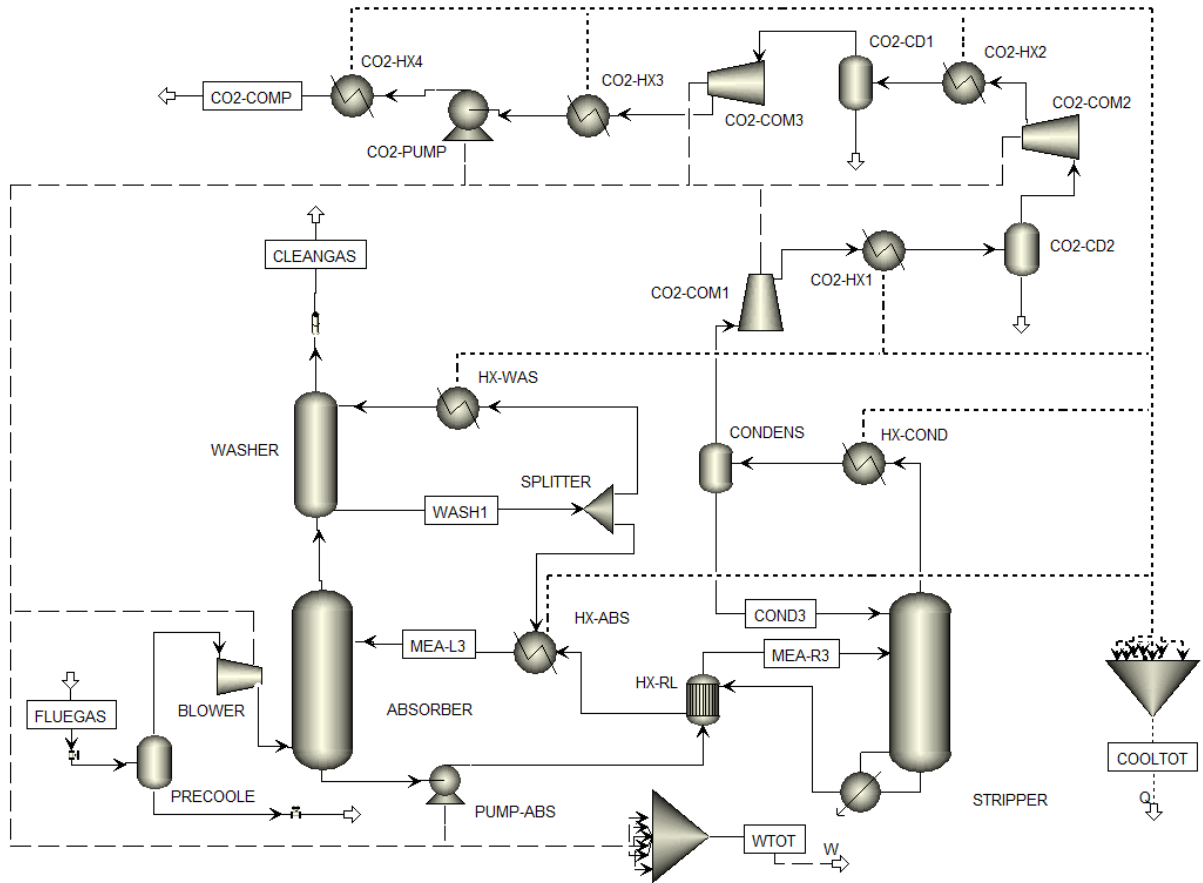
Figure 2. Flowsheet of the post-combustion CO$_2$ capture process with CO$_2$ compression.

Regarding the solvent loop, the CO$_2$-loaded MEA solution (rich solvent) is pumped to a rich-lean heat exchanger before entering the 21-stage stripper in which it is injected above the 6th stage. Indeed, the 5 upper stages of the stripping column are acting as a washing section using water condensed from the CO$_2$ exiting the stripper (stream COND3). The pressure in the stripper is set at 1.7 bar. The regenerated solvent (lean solvent) is sent back to the absorber via the rich-lean heat exchanger and is cooled down to 40°C before entering the absorber again. The gas exiting the stripper condenser undergoes four progressive pressure increase and cooling steps alternatively. Behind the first two heat exchangers, flash tanks separate CO$_2$ (gas phase) from water (liquid phase) to increase the gas purity with regards to CO$_2$. Finally, in the CO2-HX3 heat exchanger, the CO$_2$ stream is completely condensed, so the last pressure increase step is performed by pumping. At the end of the sequence, the flow is characterized by a temperature of 25°C and has been pressurized to 110 bar. The purity of the liquid CO$_2$ product reaches 99.8 wt% CO$_2$.

In agreement with a preliminary study (Léonard and Heyen, 2011), the rate-based approach is used for modeling column mass transfers. Indeed, this approach is more adapted than the equilibrium one to describe the CO$_2$ capture process since the rate-based method rigorously calculates mass and heat transfers by solving the extended Maxwell-Stefan equations, which are much more accurate at describing column internal profiles. However, in order to perform a detailed calculation of the gas-liquid mass and heat transfers, the characteristics of the column packing are required. These data have been retrieved from the Esbjerg Pilot Plant for CO$_2$ capture (Kvamsdal et al., 2011; Faber et al., 2011) and are presented along with some rate-based modeling assumptions in Table 1.

Table 1. Column packing characteristics and parameters for rate-based calculations

Parameter	Absorber	Stripper
Packing	Mellapack 2X	IMTP50, Norton, Metal
Packing height	17 m	13 m
Section diameter	1.1 m	1.1 m
Number of stages	20	21 (reboiler and washing included)
Washing section	External washing column with 2 equilibrium stages	3-stage washing section included in the stripping column
Flow model	Mixed	Mixed
Mass transfer coefficient and interfacial area correlation	Bravo et al., 1985	Onda et al., 1968
Heat transfer coefficient correlation	Chilton-Colburn method	Chilton-Colburn method
Liquid hold-up correlation	Bravo et al., 1992	Stichlmair et al., 1989
Pressure drop correlation	Confidential vendor correlation (Sulzer Chemtech)	Confidential vendor correlation (Sulzer Chemtech)
Mass transfer model	Rate-based film model, simple film in gas phase, liquid film discretized with 5-point film[a]	Rate-based film model, simple film in gas phase, liquid film discretized with 5-point film[a]

[a]Moreover, a film discretization ratio of 2 is specified, which means that the thickness of each film region is twice as large as the thickness of the next region closer to the interface.

Some chemical reactions occurring in the absorber and in the stripper are assumed to be at equilibrium, while other are kinetically limited. Table 2 gives these reactions along with their kinetic constants:

- The 3 first reactions (6-8) are reversible and their equilibrium constants are computed from Gibbs energies.

- The kinetic parameters for the CO_2 absorption reactions (9-13) describe reaction rates based on component activities according to Equation (5).

$$r = k_0 . \exp(-E_a/RT) . \prod_{i=1}^{N}(x_i \gamma_i) \tag{5}$$

A kinetic order of 1 is assumed for each reactant except water which has not been considered in the reaction kinetics. The units of the reaction rates are mol/L.s. It appears from Table 2 that the reaction describing the MEA carbamate dissociation into MEA and CO_2 considers different kinetic parameters in the absorber and the stripper. The values are provided by Aspentech (2012) based on the works of Hikita et al. (1977) and Pinsent et al. (1956). Different values are provided to describe the reaction

rate more precisely at each temperature range (40- 80°C in the absorber, 100-140°C in the stripper).

- The kinetic parameters of the Equations (14) and (15) characterizing MEA degradation have been presented in Equations (2) and (4) respectively. Please note that for Equations (14) and (15), the reaction rates are based on component concentrations and not component activities. Moreover, the unit of k_0 depends on the rate expressions given by Equations (2) and (4). Thus, the units are $(mol/L.s)/(mol/L)^{1.03}$ and $(mol/L.s)/(mol/L)$ for MEA oxidative and thermal degradation respectively.

Table 2. Reactions and rate parameters in the MEA-H_2O-CO_2-O_2 system

Equation	CO_2 capture reactions	k_0 varying unit	E_a J/mol
(6)	$OH\text{-}CH_2\text{-}CH_2\text{-}NH_3^+ + H_2O \leftrightarrow OH\text{-}CH_2\text{-}CH_2\text{-}NH_2 + H_3O^+$	-	-
(7)	$2\ H_2O \leftrightarrow H_3O^+ + OH^-$	-	-
(8)	$HCO_3^- + H_2O \leftrightarrow CO_2^{2-} + H_3O^+$	-	-
(9)	$CO_2 + OH^- \leftrightarrow HCO_3^-$	$1.33\ 10^{17}$	55 471
(10)	$HCO_3^- \rightarrow CO_2 + OH^-$	$6.63\ 10^{16}$	107 417
(11)	$OH\text{-}CH_2\text{-}CH_2\text{-}NH_2 + CO_2 + H_2O \rightarrow OH\text{-}CH_2\text{-}CH_2\text{-}NH\text{-}COO^- + H_3O^+$	$3.02\ 10^{14}$	41 264
(12)	$OH\text{-}CH_2\text{-}CH_2\text{-}NH\text{-}COO^- + H_3O^+ \rightarrow OH\text{-}CH_2\text{-}CH_2\text{-}NH_2 + CO_2 + H_2O$ (absorber)	$5.52\ 10^{23}$	69 158
(13)	$OH\text{-}CH_2\text{-}CH_2\text{-}NH\text{-}COO^- + H_3O^+ \rightarrow OH\text{-}CH_2\text{-}CH_2\text{-}NH_2 + CO_2 + H_2O$ (stripper)	$6.5\ 10^{27}$	95 384
(14)	$OH\text{-}CH_2\text{-}CH_2\text{-}NH_2 + 1.3\ O_2 \rightarrow$ $0.6\ NH_3 + 0.1\ C_5H_8N_2O + 0.1\ C_6H_{12}N_2O_2 + 0.1\ CO_2H_2 + 0.8\ CO_2 +$ $1.5\ H_2O$	$1.36\ 10^6$	55 111
(15)	$OH\text{-}CH_2\text{-}CH_2\text{-}NH_2 + 0.5\ CO_2 \rightarrow 0.5\ C_5H_{10}N_2O_2 + H_2O$	$8.00\ 10^{11}$	144 210

Finally, some assumptions were necessary to include the degradation reactions into the process model:

- Degradation reactions are included into a steady-state model of the post-combustion CO_2 capture process since dynamic simulations are not adapted to describe small modifications over long time scales (several months).

- Degradation reactions only take place in the absorption and stripping columns in order to better reflect the actual process operating conditions (degradation in other process equipment has been neglected in first approach). This is a clear improvement in comparison to the only one previous attempt to include degradation into a global process that has been identified. Indeed, Thong et al. (2012) proposed to model the degradation reactions taking place in the capture process in a separate reactor that was fed with solvent and for which the solvent residence time could be arbitrarily varied

from a few seconds to several months. This approach was not selected in the present work for three main reasons: (1) it implies to decouple the time scale of the degradation reactions from the CO_2 capture process, making it unsuited to study the influence of operating process parameters on degradation. (2) Since oxidative degradation is mass-transfer limited, it is essential to consider mass transfer limitations while modeling solvent degradation, which is not the case in the reactor model proposed by Thong et al. (2012). (3) No gas supply has been identified in the separate reactors described by Thong et al. (2012), so that the available (dissolved) oxygen is rapidly consumed and the degradation extent is severely underestimated, whatever the residence time in the degradation reactor.

- Component data for NH_3 and $HCOOH$ have been retrieved from Aspen Plus databases. Component data for HEI, HEPO and HEIA are estimated based on the component chemical structures. Moreover, these components have been defined as non-volatile to facilitate the liquid-vapor equilibria calculations in first approach. This assumption is supported by the high molecular weights of HEI, HEPO and HEIA, respectively equal to 112.13, 144.17 and 130.15 g/mol. However, the detailed influence of degradation products on solvent properties is not taken into account in the present model because very few experimental results are available in the literature about the performances of degraded solvents.

- Using Aspen's default tolerance criteria, the model perfectly converges and all mass balances are closed. However, solvent purge and make-up have been neglected in a first approach. This means that the depletion of MEA and the accumulation of degradation products are so weak that they do not prevent convergence of the tear streams in the solvent loop. However, in order to get results as precise as possible, the MEA degradation rate and the formation of degradation products are quantified by summing the composition changes occurring at each stage of the mass transfer columns. Indeed, the convergence criteria inside the rate-based columns are tighter so the component concentrations profiles in the columns are more precise than in the solvent loop.

4. Simulation study

Most existing CO_2 capture models were developed to study the influence of operating variables on the process energy requirement and they did not consider degradation reactions. The present section describes the results of the simulation study that has been performed based on the degradation model described in the previous section. As discussed, the distinctive feature of this model is its ability to evaluate the influence of process operating conditions on both the energy requirement of the process and the solvent consumption rate. After a short description of the base case configuration, the influence of the main operating variables on the process energy requirement, on the solvent degradation and on the emission of degradation products is reported. Furthermore, alternative flowsheet configurations are evaluated and optimal operating conditions are proposed that consider the process energy requirement as well as the formation of degradation products.

4.1 Base case

The results of the base case model with solvent degradation are summarized in Table 3. The reboiler heat duty predicted by the model equals 3.64 GJ/t$_{CO2}$ at a solvent flow rate of 24.48 m³/h. These values are identical to those obtained when not considering degradation

reactions since the concentrations of degradation products and the degradation rates are too weak to have any significant influence on the solvent properties, and thus on the process performances. Moreover, these values are in agreement with the experimental value (3.7 GJ/t_{CO2}) reported from the pilot plant campaign under similar conditions by Knudsen et al. (2011). Table 3 lists the formation rates of degradation products as well as the MEA degradation rate in the absorber and the stripper. The formation rates of ammonia and HEIA are reported as an indication of the oxidative and thermal degradation rates respectively. The emissions in the cleaned flue gas and in the CO_2 product streams are also reported. Since HEI, HEPO and HEIA have been assumed as nonvolatile components, there are not present in the gas streams. The liquid temperature and the vapor oxygen content at the top and bottom stages of the columns are also indicated. All degradation and emission values have been normalized by the amount of captured CO_2 which equals 1.24 t/h in the simulation.

Table 3. Degradation and emission results of the base case model.

Parameter	Unit	Absorber	Stripper	Total
MEA degradation	kg/t_{CO2}	7.95 10^{-2}	9.74 10^{-5}	7.96 10^{-2}
NH_3 formation	kg/t_{CO2}	1.33 10^{-2}	1.54 10^{-5}	1.33 10^{-2}
HEIA formation	kg/t_{CO2}	6.70 10^{-9}	5.92 10^{-6}	5.93 10^{-6}
MEA emission after washing	kg/t_{CO2}	8.74 10^{-4}	9.35 10^{-9}	8.74 10^{-4}
NH_3 emission after washing	kg/t_{CO2}	9.54 10^{-3}	2.88 10^{-3}	1.24 10^{-2}
HCOOH emission after washing	kg/t_{CO2}	1.07 10^{-4}	1.40 10^{-5}	1.21 10^{-4}
MEA loss (degradation + emission after washing)	kg/t_{CO2}	8.04 10^{-2}	9.74 10^{-5}	8.05 10^{-2}
Top stage liquid temperature	°C	57.4	96.6	-
Bottom stage liquid temperature	°C	51.2	115.6	-
Top stage O_2 content (vapor phase)	mol%	6.3	9.5 10^{-3}	-
Bottom stage O_2 content (vapor phase)	mol%	6.1	6.1 10^{-14}	-

It appears from Table 3 that more oxidative degradation products (NH_3) are formed than thermal degradation products (HEIA) over the entire process. Furthermore, MEA losses due to solvent emission are much lower than losses due to degradation. As a consequence, the MEA loss due to the oxidative degradation in the absorber (7.95 10^{-2} kg/t_{CO2}) is about 100 times higher than the sum of other MEA losses due to degradation in the stripper and solvent emission (9.71 10^{-4} kg/t_{CO2}). These results are in accordance with previous studies evidencing MEA oxidative degradation in the absorber as the main degradation pathway in industrial CO_2 capture units (Lepaumier et al., 2011).

No MEA consumption data were reported in Knudsen et al. (2011). However, previous studies using this same pilot plant reported MEA consumption rates of 2.4 and 1.4 kg/t_{CO2} respectively (Knudsen et al., 2007; Knudsen et al., 2009). Mea losses were also reported for the CSIRO Loy Yang pilot plant (Azzi et al., 2014). They ranged between 1.0 and 3.9 kg/t_{CO2}, depending on the test campaign and on the measurement method. However, Azzi et al. (2014) acknowledged that the losses they reported were partially due to plant leakages and to solvent sampling. Maybe the most precise determination of the MEA consumption rate was performed by Moser et al. (2011a) for the Niederaussem pilot plant. Indeed, this latest study could close the MEA balance within a measuring uncertainty of only 10%, so that its results can be discussed with confidence. As a consequence, they are used as pilot plant reference in the present work.

Although 3.5 times lower, the total MEA loss reported in Table 3 (0.081 kg MEA/t$_{CO2}$) is in the same order of magnitude compared with the CO_2 capture plant results reported by Moser et al. (2011a) (0.284 kg MEA/t$_{CO2}$) in the absence of degradation inhibitors. The model also predicts a lower emission of NH_3 (0.012 kg NH_3/t$_{CO2}$) than reported in Moser et al. (2011a) where the ammonia emission varied between 0.089 and 0.160 kg NH_3/t$_{CO2}$. The differences between the model predictions and the MEA loss and ammonia emission observed in pilot plant may be due to the assumptions done in first approach. For instance, the presence of SO_x and NO_x contaminants in the flue gas as well as the presence of dissolved metals in the solvent solution has been neglected in the present model. Since all these components are known to increase the degradation rate (Sexton and Rochelle, 2009), they should be considered in further model developments. Still, the present model predicts degradation and emission rates that are in the same order of magnitude and closer to pilot plant values than any previously reported predictions. Thus, this model may provide useful information about the influence of operating conditions on MEA degradation and on the emission of degradation products.

4.2 Sensitivity study

In this section, the influence of four process variables on the reboiler heat duty and the solvent loss in the CO_2 capture process is discussed. The selected process variables are the solvent flow rate, the oxygen content in the flue gas, the MEA concentration and the stripper pressure. During this sensitivity study, only one parameter is varied at a time while the others are kept constant. The influence of this variation on the reboiler duty as well as on the amine degradation and emission results is then reported.

4.2.1 Solvent flow rate

The presence of a minimum reboiler duty depending on the solvent flow rate was experimentally observed in several pilot plant studies with minimum reboiler heat duties varying between 3.5 and 3.7 GJ/t$_{CO2}$ for MEA, depending on the process configuration (e.g. Knudsen et al., 2011; Moser et al., 2011b). Indeed, the thermal energy supplied to the CO_2 capture process contributes to heat the solvent, to generate stripping steam, and to desorb CO_2. Since these three contributions vary in opposite ways with the solvent flow rate, an optimum flow rate can be identified. The same influence can be observed in the degradation model as represented in Figure 3. The base case configuration described in Section 4.1 corresponds to a reboiler duty of 3.64 GJ/t$_{CO2}$ and a solvent flow rate of 24.5 m³/h. Moreover, the rate of the MEA loss over the entire process (degradation and emission in the absorber and stripper) is also reported in this figure. The total MEA loss slightly increases with the solvent flow rate, by about 0.015 kg/t$_{CO2}$ for an increase by 4 m³/h of the solvent flow rate. This small increase of the MEA loss may be due to a higher liquid holdup in the mass transfer columns, leading to longer solvent residence times and enhanced degradation in the absorber and stripper. Furthermore, it appears that this higher MEA loss is mainly due to oxidative degradation. Indeed, the ammonia formation almost doubles from 0.009 to 0.016 kg/t$_{CO2}$ when the solvent flow rate increases from 17.7 to 30.5 m³/h. On the contrary, the formation of HEIA (representative of MEA thermal degradation) only increases from 5.5 to 6.2 10^{-6} kg/t$_{CO2}$ over the same variation range, and the MEA emission even slightly decreases from 12 to 9 10^{-3} kg/t$_{CO2}$.
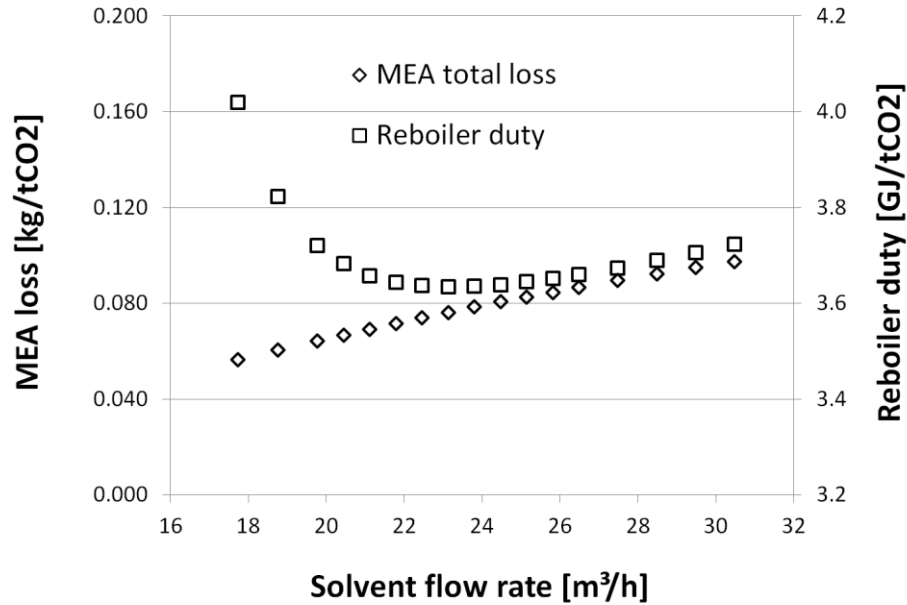
Figure 3. Influence of the solvent flow rate on the reboiler duty and the MEA loss.

4.2.2 Oxygen content

Varying oxygen contents in the flue gas may result from different operating modes of the coal (or natural gas) combustion in the power plant. In the absence of oxygen, almost no degradation is observed in Figure 4. Moreover, it appears that the MEA degradation increases linearly with the oxygen content in the flue gas since doubling the oxygen concentration from 6% (base case) to 12% causes the MEA loss to double as well, from 0.081 to 0.160 kg/t$_{CO2}$. This is related to the first-order dependency on the oxygen concentration that has been proposed in Equation (2). No significant influence of the oxygen content in the flue gas is observed on the thermal energy requirement of the process.
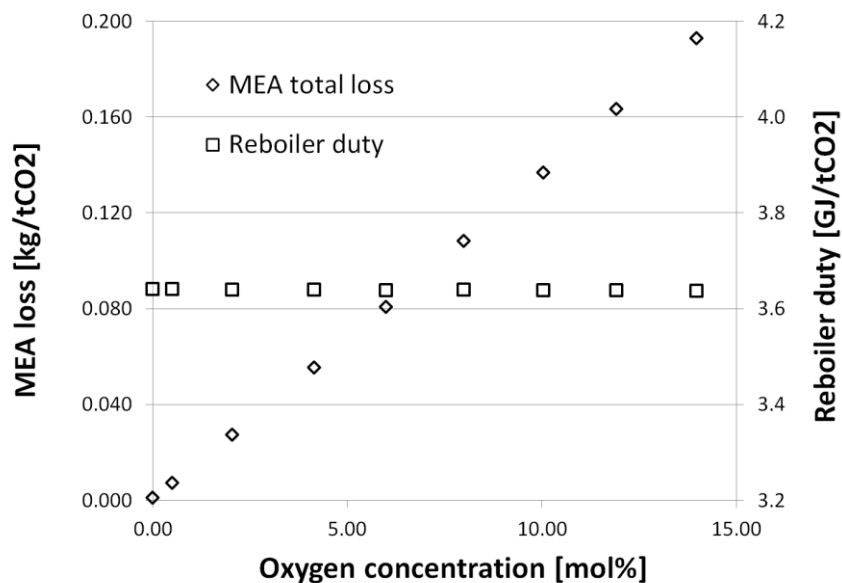
Figure 4. Influence of the oxygen concentration in the flue gas on the reboiler duty and the MEA loss.

4.2.3 MEA concentration

A higher solvent concentration increases the driving force for the CO_2 absorption and thus reduces the process thermal energy requirement. However, if we consider that oxygen also undergoes a reactive absorption like CO_2, the oxygen transfer is accelerated and the degradation increases at higher MEA concentrations as confirmed by Figure 5. It appears that increasing the MEA concentration from 30 wt% (base case) to 40 wt% approximately doubles the MEA loss from 0.081 to 0.160 kg/t_{CO2} while the reboiler heat duty is decreased by 4 % from 3.64 to 3.49 GJ/t_{CO2}. Again, the increase of the MEA loss is mostly due to oxidative degradation since the NH_3 formation doubles from 0.013 to 0.027 kg/t_{CO2} when the MEA concentration increases from 30 to 40 wt%. On the contrary, the formation of HEIA (associated to thermal degradation) and the emission of MEA both remain constant. As a consequence, concentrated MEA is not an advantageous solvent except if oxidative degradation inhibitors are added as proposed by Lemaire et al. (2011).
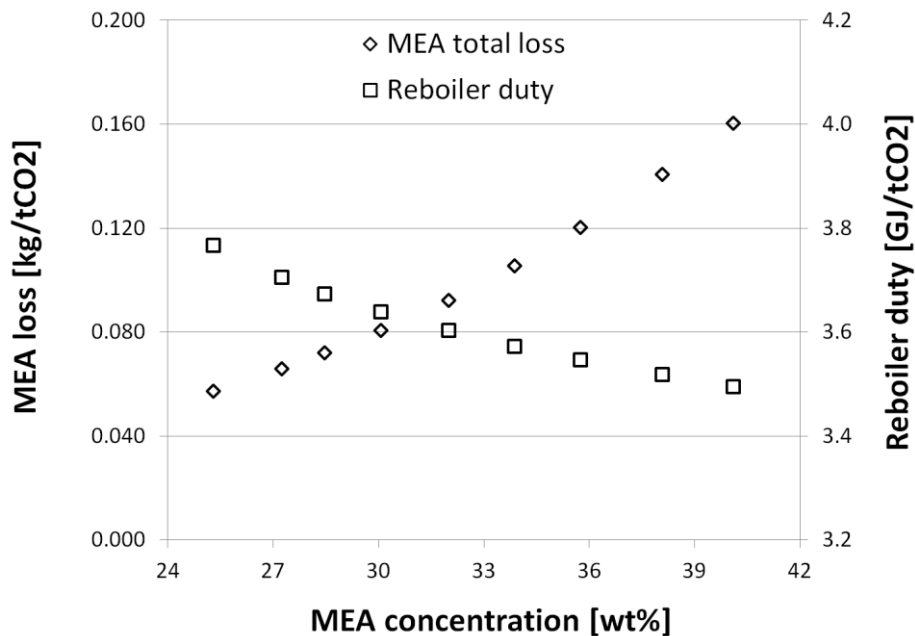
Figure 5. Influence of the MEA concentration on the reboiler duty and the MEA loss.

4.2.4 Stripper pressure

Increasing the stripper pressure from 1.7 (base case) to 4.2 bar leads to a higher bottom stage temperature (from 115 to 140 °C) and thus to an exponential increase of the MEA degradation in the stripper, from 1.0 to 5.4 10^{-4} kg/t_{CO2}. However, the influence of the stripper pressure on the MEA loss over the entire process is limited as represented in Figure 6 since the amount of degraded MEA in the stripper (maximum 5.4 10^{-4} kg/t_{CO2}) still remains two orders of magnitude below the MEA loss over the entire process (0.081 kg/t_{CO2}). Moreover, this stripper pressure increase from 1.7 to 4.2 bar also reduces the reboiler heat duty by 8.5% from 3.64 to 3.33 GJ/t_{CO2}. Thus, the model suggests that high stripping pressures are advantageous for CO_2 capture with MEA independently of degradation issues. However, the model has limitations that have to be kept in mind. For instance, the higher stripper temperature may lead to more metal ions leaching from the stripper vessel walls into the solvent solution. Back into the absorber, these metal ions may catalyze the oxidative degradation of MEA as this has been reported by Sexton and Rochelle (2009). This does not appear in the simulation since the effect of dissolved metals is not considered in the present model. In conclusion, although the

simulation evidences that thermal degradation is not so significant at high stripper pressure, other effects that are not described by the model should not be forgotten.
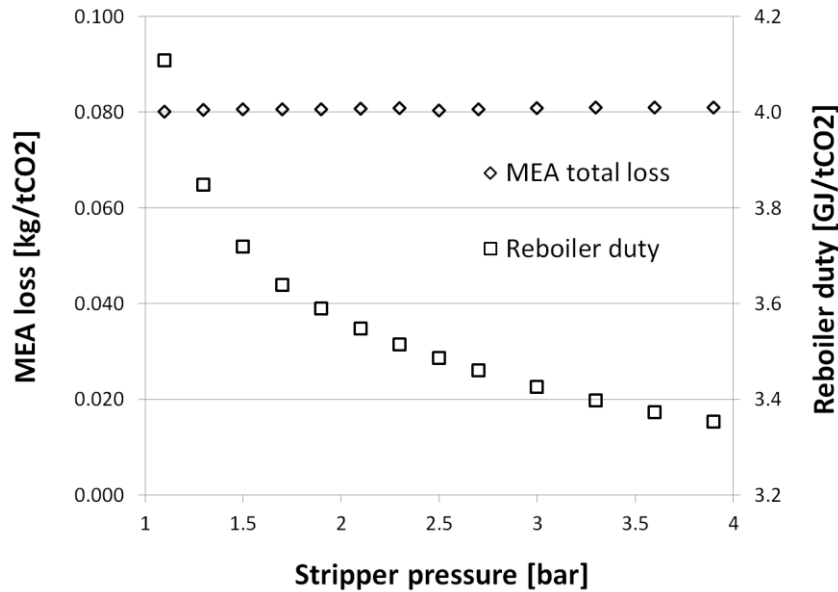

Figure 6. Influence of the stripper pressure on the reboiler duty and the MEA loss.

4.3 Alternative flowsheet configurations

Besides sensitivity studies, the modeling of alternative process configurations is a useful tool to explore potential energy savings. In the present section, the impact of two flowsheet modifications is evaluated: the absorber intercooling and the lean vapor compression. In the present work, we focus the attention on the effect they may have on solvent degradation.

4.3.1 Absorber intercooling

Since the CO_2 absorption is an exothermic reaction, reducing the average absorption temperature improves the process efficiency. To simulate the intercooling configuration, a pump-around of the liquid solvent has been modeled in the absorber column. As a consequence, the whole solvent flow is cooled down to 40°C between two absorber stages. Figure 7 confirms that it is possible to decrease the process energy consumption by about 3% (from 3.64 GJ/t$_{CO2}$ in the base case configuration to 3.54 GJ/t$_{CO2}$), depending on the location of the intercooler. Indeed, it appears that the best process efficiency is reached when the intercooler is located in the lower third of the column. Regarding the effect of the absorber intercooling on solvent degradation, the presence of an absorber intercooler reduces the mean absorption temperature, thus leading to a lower rate of oxidative degradation. Indeed, the intercooler decreases the solvent loss whatever its location since all values reported in Figure 7 are lower than the base case value without intercooling (8.1 10^{-2} kg/t$_{CO2}$). Moreover, it seems that this effect is maximal when the intercooler is located between 7th and 8th stages (starting from top) of the column (1 stage = 1 meter since the 20-meter column is discretized by 20 stages). A possible explanation would be that this location corresponds to the maximal temperature observed over the absorber profile, so the amplitude of the intercooling effect on the mean absorber temperature is maximal at that point.
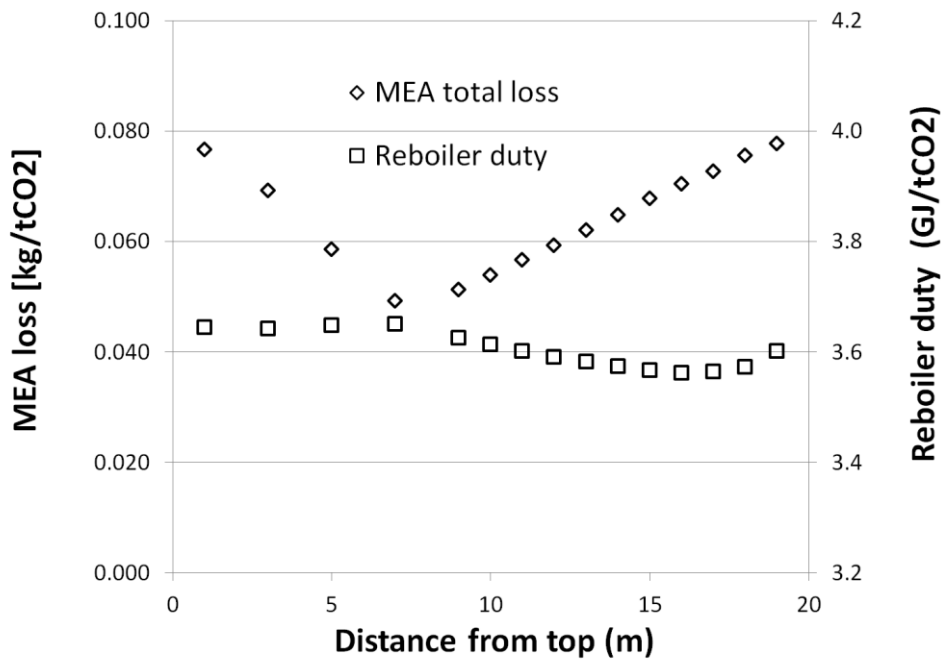
Figure 7. Influence of the absorber intercooling location on the reboiler duty and the MEA loss.

4.3.2 Lean vapor compression

As represented in Figure 8, the lean vapor compression (LVC, also called vapor recompression) consists of partially evaporating the regenerated solvent at the stripper exit in order to recover energy from the hot solvent. The generated vapor exiting the adiabatic flash tank is composed of approximately 90 wt% water and 10 wt% CO_2. This vapor is compressed and recycled to the stripper where it acts as auxiliary stripping steam and thus allows a reduction of the reboiler duty. Some water is mixed to the generated vapor flow to desuperheat it before recompression, so the vapor temperature does not exceed 125°C at the stripper inlet.
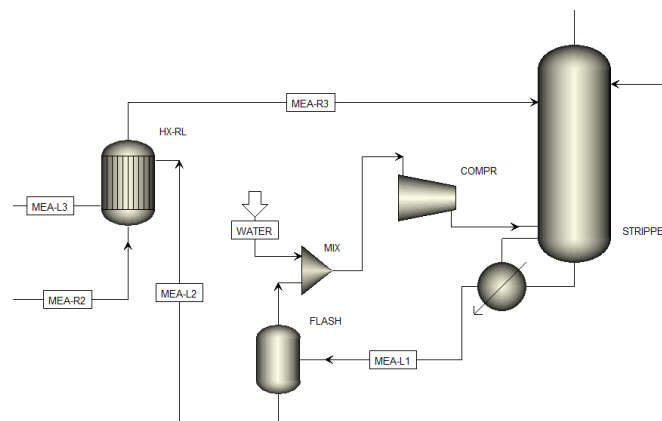
Figure 8. Flowsheet of the lean vapor compression

The influence of the flash tank pressure on the reboiler heat duty and on the MEA loss is reported in Figure 9. If the flash tank is operated at 0.9 bar, the reboiler heat duty is reduced by 18% from 3.64 GJ/t_{CO2} in the base case configuration to 2.98 GJ/t_{CO2}. However, the vapor

recompression implies a higher electricity demand in the process. The concept of exergy may be helpful to compare the improvement brought by this flowsheet modification. Indeed, the exergy is defined as the maximum work that can be produced during a process that brings the system to equilibrium with its thermodynamic reference state (atmospheric pressure, 288.15 K). The energy provided in the form of electricity or mechanical work is equal to the exergy, while the energy provided in the form of heat is multiplied by the Carnot efficiency to convert it into exergy. Based on a hot steam temperature of 443 K in the reboiler and a cold reference of 288.15 K, the Carnot efficiency equals 35%. Finally, the vapor recompression induces a reduction of the process exergy requirement by 9.5% from 1.60 GJ/t_{CO2} in the base case configuration down to 1.45 GJ/t_{CO2}. Moreover, it does not seem to have any impact on the solvent degradation rate, so these results suggest that this process modification should be systematically implemented in the CO_2 capture process with MEA.
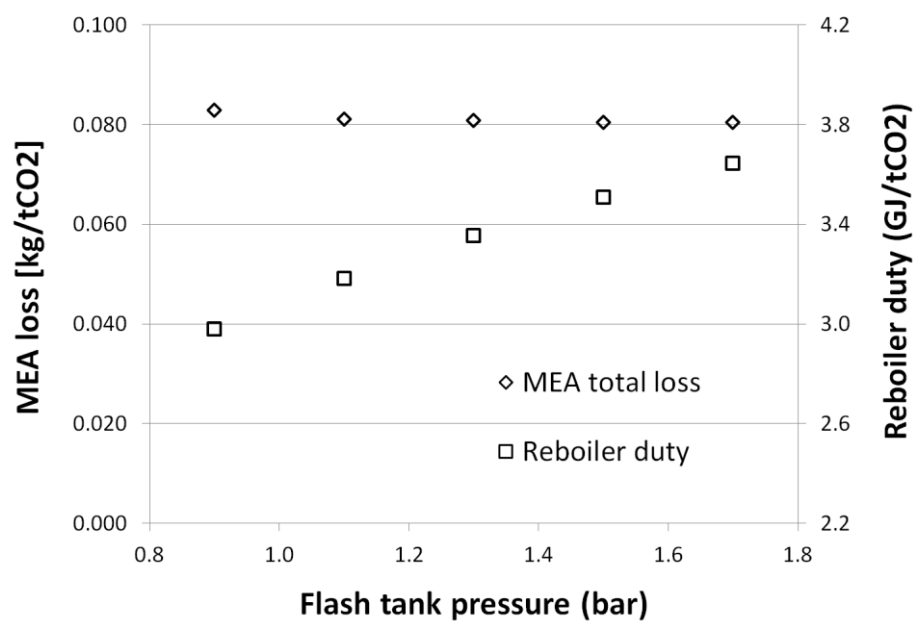

Figure 9. Influence of the flash tank pressure for lean vapor compression on the reboiler duty and the MEA loss.

4.4 Optimal operating conditions

Based on the sensitivity analysis and on the process improvements that have been studied, it is possible to propose optimal operating conditions for the post-combustion CO_2 capture process with MEA. Following assumptions are considered:

- The flue gas composition cannot be modified, so the oxygen content is fixed at 6 vol%.

- The MEA concentration is kept equal to 30 wt%, although this could be increased to 40 wt% if efficient degradation inhibitors are available.

- The stripper pressure is set at 1.7 bar and the solvent flow rate is optimized at 24.5 m³/h based on the design data used in the present model.

- Both the absorber intercooling and the lean vapor compression are implemented in the optimal configuration. The intercooler is located between the 16th and the 17th stages (starting from top) of the 20-stage absorber and the flash tank pressure is set at 0.9 bar for the lean vapor compression.

As a result, the reboiler duty decreases by 19.7% from 3.64 GJ/t_{CO2} in the base case configuration to 2.92 GJ/t_{CO2} in the optimal configuration. The reduction of the reboiler duty is mainly due to the lean vapor compression and it is coherent with the value of about 2.90 GJ/t_{CO2} reported by Knudsen et al. (2011) for pilot plant experiments combining absorber intercooling and lean vapor compression. Overall, the process exergy requirement decreases by 10.8%, from 1.60 GJ/t_{CO2} in the base case configuration to 1.43 GJ/t_{CO2} in the optimal configuration. Moreover, an 11.1%-reduction of the MEA loss could be achieved, from 0.081 to 0.072 kg/t_{CO2}. This improvement seems to be related to the absorber intercooling that decreases the mean absorber temperature and thus reduces the extent of oxidative degradation. However, further model refinements and validation with pilot plant data are necessary to confirm this explanation since no degradation data are available for a pilot plant operating with lean vapor compression and absorber intercooling.

5.   Conclusion

Most existing models of the CO_2 capture process have been developed to evaluate the process energy requirement in order to reduce the cost of the technology. However, they neglect solvent degradation and its consequences on the process, which are one of the most important operational drawbacks of the post-combustion CO_2 capture with amines. Thus, the objective of the present work was to integrate own experimental results of solvent degradation into a global process model. After the description of the model, a simulation study has evidenced the potential of such approach for the CO_2 capture process. Combining a sensitivity study with some process improvements made to the base case configuration, the process operating conditions that increase solvent degradation could be identified. The reboiler duty was reduced by almost 20% and the solvent consumption rate by 11% by using a single tool. A cost estimation of the impact of degradation can be calculated using similar assumptions to Abu Zahra et al. (2007b): CO_2 capture unit treating the flue gas of a 600 MW_e coal power plant, capture rate of 408 t_{CO2}/h, plant run time of 7500 h/year and MEA price of 1 €/ton. In this case and with a MEA loss of 0.072 kg/t_{CO2} as achieved in section 4.4, the cost of the MEA consumption equals 0.22 M€/year, or 1.3% of the total CO_2 capture Opex. When using a degradation rate of 0.284 kg/t_{CO2} as reported by Moser et al. (2011a), the MEA consumption cost equals 4.9% of the total CO_2 capture Opex.

These results evidence that although the reboiler duty prediction is very close to pilot plant results (2.92 versus 2.90 GJ/t_{CO2}, see section 4.4), the model still underpredicts the solvent consumption (0.081 versus 0.284 kg/t_{CO2}, see section 4.1). Further effects neglected in first approach would most probably lead to degradation rates that are closer to experimental results. For instance, the model may be adapted to include the effect of dissolved metals as intensively studied by Voice (2013) who proposed a kinetic expression for oxidative degradation in the presence of metal ions. Other improvements would be to consider flue gas contaminants like SO_x and NO_x, to include the effect of degradation on solvent performances, and to consider degradation reactions inside additional process blocs (e.g., Voice (2013) has shown that oxidative degradation also significantly occurs in the cross heat exchanger). Similarly, the influence of degradation inhibitors as studied in Léonard et al. (2014e) should also be modeled if such inhibitors are used to prevent MEA oxidative degradation.

In conclusion, solvent degradation appears as a complex phenomenon which requires further research to be fully understood. The model developed in the present work proposes a first approach for considering solvent degradation as a part of the CO_2 capture process. Its main purpose is to give a better understanding of the influence of process operating conditions on solvent degradation. So far as we know, this is the first time that the degradation rate of a pilot plant can be predicted so closely, although further model refinements are necessary to improve the prediction. Moreover, the model offers pathways to decrease both the process energy consumption and the emission of solvent degradation products. As a consequence, the CO_2 capture may operate in a more efficient and more sustainable way. The methodology developed for the case of monoethanolamine may also be extended to other promising solvents. Finally, such model may provide a useful tool for the design of large-scale CO_2 capture plants to facilitate the deployment of CO_2 capture, re-use and storage technologies (CCUS).
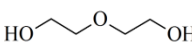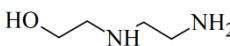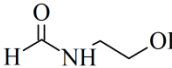
Acknowledgements
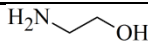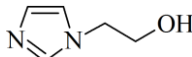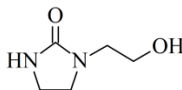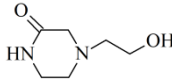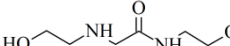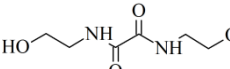
References

Abu Zahra M., Schneiders L., Niederer J., Feron P., Versteeg G., 2007a. CO_2 capture from power plants. Part I. A parametric study of the technical performance based on monoethanolamine. International Journal of Greenhouse Gas Control 1, 37-46.

Abu Zahra M., Schneiders L., Niederer J., Feron P., Versteeg G., 2007b. CO_2 capture from power plants. Part II. A parametric study of the economical performance based on mono-ethanolamine. International Journal of Greenhouse Gas Control 1, 135-42.

Aspentech, 2012. Rate-based model of the CO_2 capture process by MEA using Aspen Plus. Aspen Plus V8.0 support files.

Azzi M., Tibbett A., Halliburton B., Element A., Artanto Y., Meuleman E., Feron P., 2014. Assessing atmospheric emissions from amine-based CO_2 post-combustion capture processes and their impacts on the environment - A case study. Volume 1: Measurement of emissions from a monoethanolamine-based post-combustion CO_2 capture pilot plant. Technical report. Global Carbon Capture and Storage Institute, May 2014.

Bloomberg, 2013. The Future of China's Power Sector. New Energy Finance report. Bloomberg Finance L.P.

Bravo J., Rocha J., Fair J., 1985. Mass-transfer in Gauze packings. Hydrocarbon Process 64, 91-5.

Bravo J., Rocha J., Fair J., 1992. A comprehensive model for the performance of columns containing structured packings. IChemE. Symp. Ser. 128, A439.

Faber R., Köpcke M., Biede O., Knudsen J., Andersen J., 2011. Open-loop step responses for the MEA post-combustion capture process: Experimental results from the Esbjerg pilot plant. Energy Procedia 4, 1427-34.

Freguia S., Rochelle G., 2003. Modeling of CO_2 capture by aqueous monoethanolamine. AIChE Journal 49 (7), 1676-86.

Goff G., 2005. Oxidative degradation of aqueous monoethanolamine in CO_2 capture processes: iron and copper catalysis, inhibition, and O_2 mass transfer. Ph.D. thesis at the University of Texas at Austin, 76-119.

Hikita H., Asai S., Ishikawa H., Honda M., 1977. The kinetics of reactions of carbon dioxide with monoethanolamine, diethanolamine, and triethanolamine by a rapid mixing method. Chemical Engineering Journal 13 (1), 7-12.

IEA, 2013. World Energy Outlook 2013, Factsheet. International Energy Agency, OECD/IEA, Paris.

Karimi M., Hillestad M., Svendsen H., 2011a. Investigation of intercooling effect in CO_2 capture energy consumption. Energy Procedia 4, 1601-1607.

Karimi M., Hillestad M., Svendsen H., 2011b. Capital costs and energy considerations of different alternative stripper configurations for post combustion CO_2 capture. Chemical Engineering Research and Design 89, 1229-36.

Knudsen J., Jensen J., Vilhelmsen P., Biede O., 2007. First year operation experience with a 1 t/h CO_2 absorption pilot plant at Esbjerg coal-fired power plant. Proceedings of European Congress of Chemical Engineering (ECCE-6), Copenhagen, 16-20 September 2007.

Knudsen J., Vilhelmsen P., Jensen J., Biede O., 2009. Experience with CO_2 capture from coal flue gas in pilot scale: Testing of different amine solvents. Energy Procedia 1, 783-790.

Knudsen J., Andersen J., Jensen J., Biede O., 2011. Evaluation of process upgrades and novel solvents for the post combustion CO_2 capture in pilot-scale. Energy Procedia 4, 1558-65.

Kvamsdal H., Haugen G., Svendsen H., Tobiesen A., Mangalapally H., Hartono A., Mejdell T., 2011. Modelling and simulation of the Esbjerg Pilot Plant using the Cesar 1 solvent. Energy Procedia 4, 1644-51.

Lemaire E., Bouillon P.A., Gomez A. Kittel J., Gonzales S., Carrette P.-L., Delfort B., Ougin P., Alix P., Normand L., 2011. New IFP optimized first generation process for post-combustion CO_2 capture: HiCapt+TM. Energy Procedia 4, 1361-68.

Léonard G, Heyen G, 2011. Modeling post-combustion CO_2 capture with amine solvents. Computer Aided Chemical Engineering 29, 1768-72.

Léonard G., Cabeza Mogador B., Belletante S., Heyen G., 2013. Dynamic modelling and control of a pilot plant for post-combustion capture. Computer Aided Chemical Engineering 31, 451-6

Léonard G., 2013. Optimal design of a CO_2 capture unit with assessment of solvent degradation. Ph.D. thesis at the University of Liège, 112-20.

Léonard G., Toye D., Heyen G., 2014a. Relevance of accelerated conditions for the study of monoethanolamine degradation in post-combustion CO_2 capture. Canadian Journal of Chemical Engineering, in press. DOI: 10.1002/cjce.22094.

Léonard G., Toye D., Heyen G., 2014b. Experimental study and kinetic model of monoethanolamine oxidative and thermal degradation for post-combustion CO_2 capture. International Journal of Greenhouse Gas Control 30, 171. DOI: 10.1016/j.ijggc.2014.09.014.

Léonard G., Crosset C., Dumont M-N., Toye D., 2014c. Designing large-scale CO_2 capture units with assessment of solvent degradation. Energy Procedia, in press.

Léonard G, Toye D, Heyen G, 2014d. Assessment of Solvent Degradation within a Global Process Model of Post-Combustion CO_2 Capture. Computer Aided Chemical Engineering 33, 13-8.

Léonard G., Voice A., Toye D., Heyen G., 2014e. Influence of dissolved metals and oxidative degradation inhibitors on the oxidative and thermal degradation of monoethanolamine for post-combustion CO_2 capture. Industrial & Engineering Chemistry Research 53 (47), 18121-9.

Lepaumier H., da Silva E., Einbu A., Grimstvedt A., Knudsen J., Zahlsen K., Svendsen H., 2011. Comparison of MEA degradation in pilot-scale with lab-scale experiments. Energy Procedia 4, 1652-9.

Mertens J., Lepaumier H., Desagher D., Thielens M.-L., 2013. Understanding ethanolamine (MEA) and ammonia emissions from amine based post combustion carbon capture: Lessons learned from field tests. International Journal of Greenhouse Gas Control 13, 72-7.

Moser P., Schmidt S., Stahl K., 2011a. Investigation of trace elements in the inlet and outlet streams of a MEA-based post-combustion capture process - Results from the test programme at the Niederaussem pilot plant. Energy Procedia 4, 473-9.

Moser P., Schmidt S., Sieder G., Garcia H., Stoffregen T., 2011b. Performance of MEA in a long-term test at the post-combustion capture pilot plant in Niederaussem. International Journal of Greenhouse Gas Control 5, 620-7.

Onda K., Takeuchi H., Okumoto Y., 1968. Mass transfer coefficients between gas and liquid phases in packed columns. J. Chem. Eng. Jpn. 1, 56-62.

Pinsent B., Pearson L., Roughton F., 1956. The kinetics of combination of carbon dioxide with hydroxide ions. Transactions of the Faraday Society 52, 1512-20.

Plaza J., Van Wagener D., Rochelle G., 2010. Modeling CO_2 capture with aqueous monoethanolamine. International Journal of Greenhouse Gas Control 4, 161-6.

Sexton A, Rochelle G., 2009. Catalysts and inhibitors for oxidative degradation of monoethanolamine. International Journal of Greenhouse Gas Control 3, 704-11.

Stichlmair J., Bravo J., Fair J., 1989. General model for prediction of pressure drop and capacity of countercurrent gas/liquid packed columns. Gas Separation and Purification 3 (1), 19-28.

Thong D., Dave N., Feron P., Azzi M, 2012. Estimated emissions to the atmosphere from amine based PCC processes for a black coal fired power station based on literature and modelling. Deliverable 3.1 for Australian National Low Emissions Coal Research and Development, Environmental Impact of Amine-based CO_2 Post-combustion Capture (PCC) Process. CSIRO - Advanced Coal Technology Portfolio.

Voice A., 2013. Amine Oxidation in Carbon Dioxide Capture by Aqueous Scrubbing. Ph.D. thesis at the University of Texas at Austin.

Appendix. Main products identified in GC spectra of degraded MEA samples (Léonard et al., 2014a)

	Compound		Structure	Retention time (min)	Type
1	MEA	monoethanolamine		7.6	Start amine
2	DEG	diethylene glycol		15.0	Internal standard
3	HEEDA	*N*-(2-hydroxyethyl)ethylenediamine		17.0	Quantified
4	HEF	*N*-(2-hydroxyethyl)formamide		21.1	Identified
5	OZD	2-oxazolidinone		22.5	Quantified
6	HEI	*N*-(2-hydroxyethyl)imidazole		24.9	Quantified
7	HEIA	*N*-(2-hydroxyethyl) imidazolidinone		31.5	Quantified
8	HEPO	4-(2-hydroxyethyl)piperazine-2-one		34.3	Quantified
9	HEHEAA	*N*-(2-hydroxyethyl)-2-(2-hydroxyethylamino)acetamide		36.8	Identified
10	BHEOX	*N,N'*-bis(2-hydroxyethyl)oxamide		38.7	Quantified